Available online at www.sciencedirect.com

ScienceDirect

Ceramics International 39 (2013) 8853–8859

CERAMICS INTERNATIONAL

www.elsevier.com/locate/ceramint

Synthesis of $La_2Mo_2O_9$ powders with nanodomains using polyol procedure

Houssem Sellemi[a,b], Sandrine Coste[a], Amor Ben Ali[b], Richard Retoux[c], Leila Samia Smiri[b], Philippe Lacorre[a,*]

[a]LUNAM Université, Université du Maine, UMR CNRS 6283, Institut des Molécules et Matériaux du Mans (IMMM), département Oxydes et Fluorures, Avenue Olivier Messiaen, 72085 Le Mans Cedex, France

[b]Synthèse et structure de nanomatériaux UR11ES30, Université de Carthage, Faculté des Sciences de Bizerte, 7021 Jarzouna, Tunisia

[c]Laboratoire CRISMAT UMR CNRS 6508, ENSICAEN, 6 boulevard Maréchal Juin, 14050 Caen Cedex, France

Received 14 January 2013; received in revised form 18 April 2013; accepted 22 April 2013
Available online 10 May 2013

Abstract

Powders of oxide-ion conductor $La_2Mo_2O_9$ presenting nanodomains were synthesized by using polyol processes. The influence of different process parameters on the structure and particles morphology was determined. By the classical polyol process, whatever the polyol solvent used (ethylene glycol, diethylene glycol, 1,2-propanediol and tetraethylene glycol) platelet particles with dimensions of few hundred nanometers long and around twenty nanometers thick were observed, as agglomerates of small sub-particles. Only with diethylene glycol, pure $La_2Mo_2O_9$ was obtained, whereas with microwave assistance, ethylene glycol also leads to pure product. For both ethylene and diethylene glycol solvent, the microwave assisted process resulted in either agglomerates or desert roses conglomerates after heat treatments at 500 °C for 5 min or 2 h. Specific surface areas, ranging between 23 and 36 $m^2\ g^{-1}$, have been measured for pure $La_2Mo_2O_9$ powders.

Keywords: A. Powders: chemical preparation; B. Electron microscopy; B. Microstructure-final; B. X-ray methods; $La_2Mo_2O_9$

1. Introduction

The current concern for clean energy generation has triggered the development of fuel cells, among which solid oxide fuel cells (SOFCs) are particularly attractive for domestic power and heat co-production. A current challenge is, by finding the most appropriate materials, to lower the operating temperature of such devices in order to reduce the costs and minimize reactivity between the cell core components [1]. $La_2Mo_2O_9$ and derived LAMOX oxide-ion conductors might be suitable candidates due to their high ionic conductivity [2]. $La_2Mo_2O_9$ presents two polymorphic phases: at low temperature the less conducing ordered α phase is monoclinic, while at high temperature the highly conducing disordered β phase is cubic [3]. The α-β first order phase transition, which occurs at about 580 °C, is detrimental to the mechanical stability. However it can be overcome by appropriate cationic substitutions which stabilize the β-phase down to room temperature [4]. Nevertheless the instability of these molybdates under reducing atmosphere, as well as the very good catalytic properties of $La_2Mo_2O_9$ for the oxidation of propane, make them more suitable as core cell materials for single chamber SOFCs [5]. Indeed their reduction generates the appearance of electronic conductivity, turning them into mixed ionic-electronic conductors (MIEC), which becomes an advantage for application as anode materials in conventional double chamber SOFCs [6]. As a matter of fact, the amorphous reduced form $La_2Mo_2O_{7-\delta}$ has been shown to be a performing, sulphur-tolerant, anode material [7].

The studies summarized above show that $La_2Mo_2O_9$ based derivatives have good potentialities for applications as SOFC core materials. Among them, the use as anode materials in conventional SOFC design is the most promising. It requires the elaboration of porous layers with as small particles as possible in order to optimize the gas contact with the MIEC surface.

The most common synthesis method to prepare $La_2Mo_2O_9$ and derivatives is the solid state route, from which most of the properties of these materials have been studied. Although very simple, this method is both time and energy consuming, since optimal synthesis temperatures are close to 1000 °C for at least

*Corresponding author. Tel.: +33 2 4383 2643; fax: +33 2 4383 3506.
E-mail addresses: sellemi.houssem@gmail.com (H. Sellemi), sandrine.coste@univ-lemans.fr (S. Coste), Amor.BenAli@fsb.rnu.tn (A. Ben Ali), richard.retoux@ensicaen.fr (R. Retoux), lsmiri@gmail.com (L.S. Smiri), philippe.lacorre@univ-lemans.fr (P. Lacorre).

0272-8842/$ - see front matter © 2013 Elsevier Ltd and Techna Group S.r.l. All rights reserved.
http://dx.doi.org/10.1016/j.ceramint.2013.04.076

several hours. Moreover, the large particles obtained by this way are inappropriate for use in the above-mentioned application unless reduced in size, but partly efficient grinding generally induces the introduction of impurities detrimental to the materials properties. In order to overcome this problem, efficient synthetic methods have already been proposed, such as freeze drying [8] or spray pyrolysis [9]. However these methods remain relatively costly due to the requested equipment. Other, more classical ways have been used, such as the citrate method [10], a Pechini or modified Pechini route [11–14], the microwave assisted method [15] and the EDTA complexation method [16].

Our aim with the current work is to develop convenient methods which are not too costly, in order to prepare powders with large specific surface area and different morphologies, and to elaborate coatings, both to be used in suitable applications. For this purpose we present here another preparation method, the polyol process, which can lead to various microstructures [17–19], control the particles size [20], and lower the temperature of the heat treatment —generally necessary as a final step when soft chemistry is used.

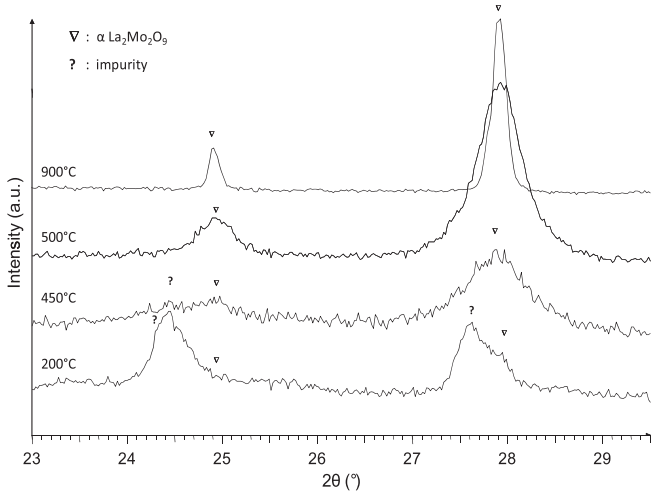

Fig. 1. XRD diagrams of the peak around 2θ=24.5° and of the most intense pseudo-cubic (210) peak recorded on the powder obtained by the polyol process (P_{DEG}) followed by heat treatment at 200 °C for 2 h, at 450 °C for 5 min, at 500 °C for 5 min and at 950 °C for 2 h.

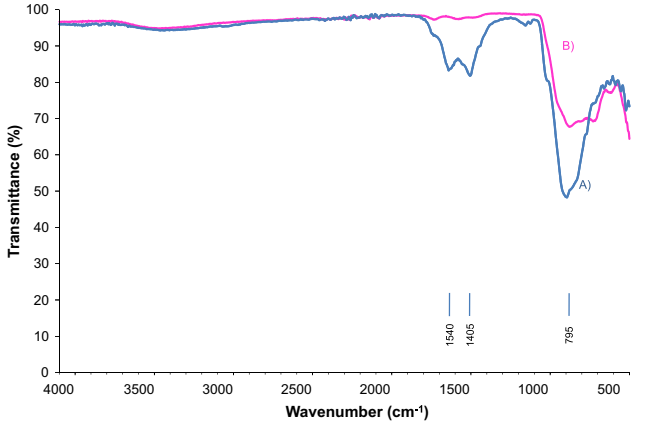

Fig. 2. FTIR spectra of powders obtained by the polyol process (P_{DEG}) and heated at (A) 450 °C or (B) 500 °C for 5 min.

2. Material and methods

The polyol process has been investigated through a classical refluxing route or, for comparison, through a microwave-assisted process. In both cases, following thermal treatments have been realized.

2.1. Polyol process

Precursor salts, $La(CH_3CO_2)_3 \cdot 1{,}5\ H_2O$ (Alfa Aesar, 99.99%) and $(NH_4)_2Mo_2O_7$ (Alfa Aesar, Mo 56.5%) were dissolved in 30 mL of glycol ([La+Mo]=0.2 mol L^{-1}) in the appropriate ratio to give a composition corresponding to $La_2Mo_2O_9$. Four glycols solvents have been tested: ethylene glycol (EG) (Acros Organics, 99%), diethylene glycol (DEG) (Acros Organics, >99%), 1,2-propanediol (PEG) (Acros Organic, 97%) and tetraethylene glycol (TEG) (Acros Organics, 99.5%).

The resulting mixture was then heated to reflux under mechanical stirring for 3 h. During this process, the initial precursor dissolved totally and the color of the obtained solution gradually changed to white color, and then a white–gray precipitate appeared. After cooling, the obtained precipitate was washed and dried in air at 60 °C for 24 h. The obtained powders are called precursors hereafter. Finally, ultrafine $La_2Mo_2O_9$ powders were obtained by flash heat treatments for 5 min or 2 h in a muffle furnace preheated at a fixed temperature ranging from 200 to 900 °C. The aim of this flash heat treatment was to avoid any important growth of the grain size.

2.2. Microwave-assisted process

$La_2Mo_2O_9$ phase was obtained from the solvothermal reaction by using a microwave oven (CEM Mars). A mixture of $La(CH_3CO_2)_3 \cdot 1{,}5H_2O$ (Alfa Aesar, 99.99%) and $(NH_4)_2Mo_2O_7$ (Alfa Aesar, 99.99%) was dissolved in 15 ml of DEG or EG ([La+Mo]=0.2 mol L^{-1}), and placed in a Teflon autoclave and heated at 180 °C for 1 h. After cooling, a precipitate was obtained. The same treatments, as for the classical polyol process, were carried out on the precipitate to obtain the $La_2Mo_2O_9$ powders.

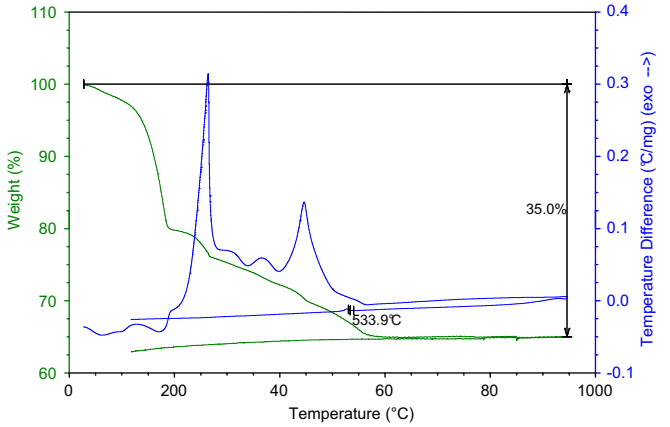

Fig. 3. DTA-TG of the dried precipitate (P_{DEG}) obtained by the polyol process in DEG.

2.3. Characterization techniques

The phase purity of the obtained powders was checked by X-Ray powder Diffraction (XRD) analysis. Patterns were recorded at room temperature on a PANalytical θ/θ Bragg–Brentano X'pert MPD PRO diffractometer (CuKα radiation) equipped with the X'Celerator detector. The diagrams were collected in 10–60° scattering angle range.

Fourier Transformed InfraRed (FTIR) spectra were collected in air with an Alpha Bruker spectrometer equipped with an ATR sampling module. Each spectrum was obtained in the 4000–400 cm^{-1} range.

Thermal analyses were performed on raw precipitates with a TGA/DTA Q600 SDT TA Instruments apparatus (Pt crucibles, Al_2O_3 as a reference) under air flow (100 mL/min). Thermograms were collected between room temperature and 950 °C with a heating/cooling rate of 10 °C min^{-1}.

Carl Zeiss Supra 55 (Oberkochen, Germany) high resolution scanning electron microscope (SEM) equipped with EDS was used to investigate the morphology.

The transmission electron microscopy (TEM) study was performed using a 200 kV JEOL 2010 FEG transmission electron microscope fitted with a double tilt sample holders (tilts ±42°). Specimens for TEM observations were prepared by crushing powdered samples in ethanol. After dispersion of the crystallites a drop of the suspension is deposited and dried onto a carbon coated copper grid.

The specific surface area measurements were realized according to the BET method with a Micromeritics Tristar II apparatus.

3. Results and discussion

3.1. Effect of heat treatment temperature

This part deals with the powders obtained by the common polyol process (without microwave assistance) in the DEG as solvent. Precursor powder (P_{DEG}) was treated at a fixed temperature in the range 200–900 °C for annealing time of 5 min or 2 h. XRD patterns of the precursor, and of the precursor annealed at 200 °C for 2 h present mainly two peaks around 24.5 and 27.8° (in 2θ) (Fig. 1). These peaks are still present after annealing at 450 °C, whereas they disappear after a flash heat treatment at 500 °C for 5 min. Moreover, after annealing at 500 °C for 5 min, no organic groups are detected by FTIR (Fig. 2). Bands around 1540 and 1405 cm^{-1} and probably around 630 cm^{-1}, that could be attributed to nitro groups (NO_2), are observed after annealing at 450 °C and have quite totally disappeared after a flash heat treatment at 500 °C for 5 min. The other bands under 1000 cm^{-1} correspond to inorganic groups (metal-oxygen bonds). According to these results, the optimal thermal condition in order to obtain pure $La_2Mo_2O_9$ powders with a minimal grain size seems to be a flash heat treatment at 500 °C for 5 min. These results are in agreement with the DTA-TG results (Fig. 3) as the entire weight loss of about 35% is reached at around 550 °C. The slight difference between this temperature and the one obtained by flash heat treatment can be explained by a difference in temperature between the two furnaces as well as the difference in kinetics between these two heat treatments.

By XRD, as expected, a decrease of the full width at half maximum (FWHM) partially or totally due to an increase of the crystallite size can be observed mainly with temperature increase and more slightly with annealing time, the impact of time being more important at 500 °C than at 600 °C (Fig. 4). The 2θ evolution of the observed FWHM of the most intense peaks, assuming each observed peak as a single (hkl) reflexion (cubic setting), is presented in Fig. 5. The same evolutions for the α and β-$La_2Mo_2O_9$ phases obtained by the solid state route have been added for comparison. Indeed, one of the differences between the monoclinic and cubic phase XRD diagrams is the presence of small superstructure peaks in the monoclinic α phase. As the FWHM of the peak is very important, these superstructure peaks cannot be evidenced. However another difference originates from the monoclinic peak splitting, which is more or less pronounced depending on the diffraction planes. It was used to identify the nature of the $La_2Mo_2O_9$ phases obtained by the polyol process. The irregular evolution of the FWHM with the diffraction angle, very similar to that of α $La_2Mo_2O_9$ phase obtained by solid state route, indicates that all the samples obtained by the common polyol process are α

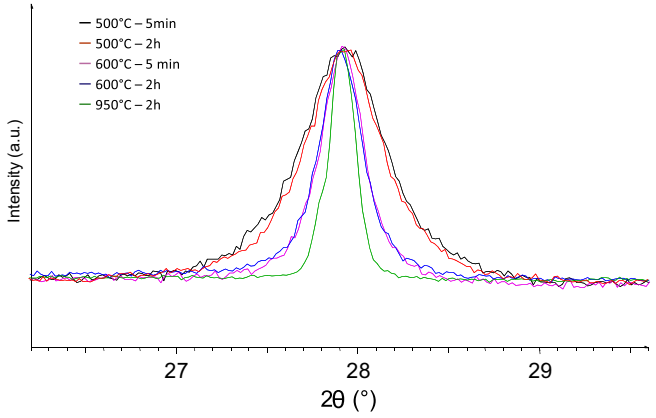

Fig. 4. XRD diagrams of the most intense pseudo-cubic (210) peak of the dried precipitate (P_{DEG}) obtained by the polyol process and heated at 500 °C for 5 min and 2 h, at 600 °C for 5 min and 2 h, and at 950 °C for 2 h.

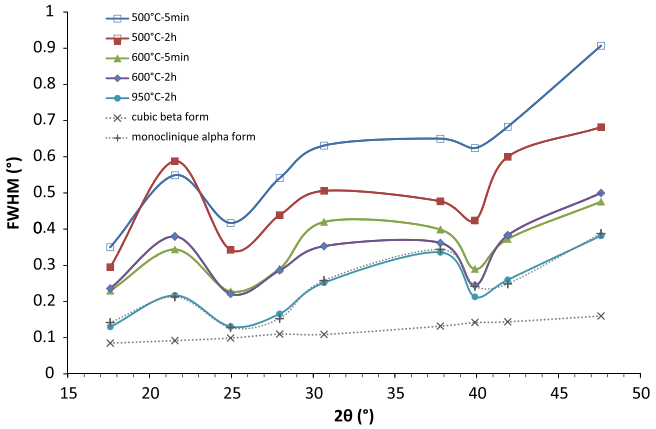

Fig. 5. Observed FWHM of XRD peaks of the polyol-process made powders heated at 500 °C for 2 h and 5 min, at 600 °C for 2 h and 5 min, and at 950 °C for 2 h.

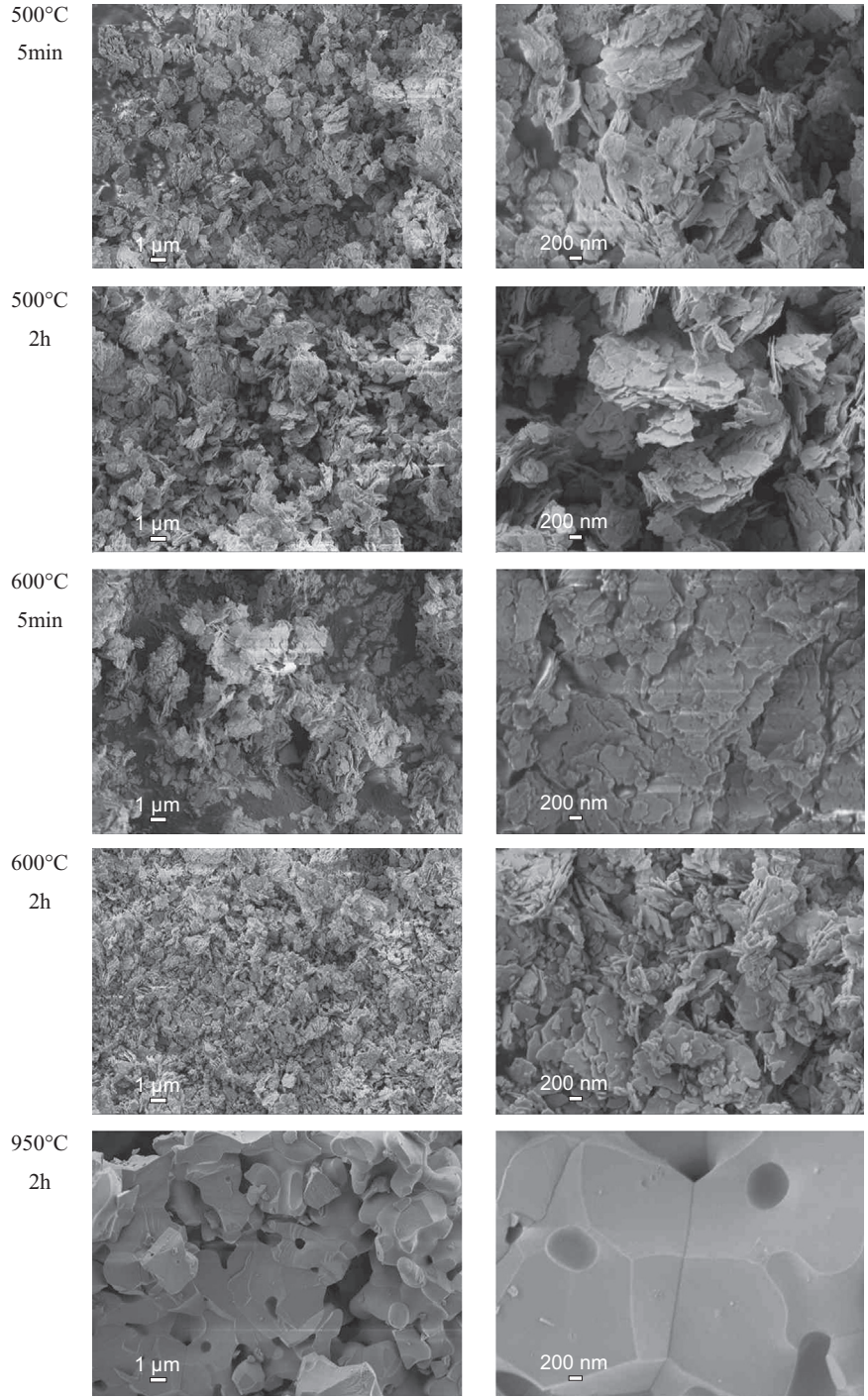

Fig. 6. SEM images of the polyol-process made powders heated at 500 °C for 5 min and 2 h, at 600 °C for 5 min and 2 h, and at 950 °C for 2 h.

type in nature. This is in agreement with the exothermic peak observed by DTA at around 534 °C while cooling down (see Fig. 3), suggesting that at least a part of the β-$La_2Mo_2O_9$ phase transforms into the α-$La_2Mo_2O_9$ phase [3,21,22].

The crystallite size has been estimated, from XRD patterns, according to the Scherrer equation (the contribution of the apparatus on the FWHM being deduced). From the thinner diffraction peak at about 2θ=25°, the crystallite size is around 23 nm after a flash heat treatment at 500 °C for 5 min, and around 143 nm after a heat treatment at 950 °C for 2 h. No effect of the grain size on the stabilization of the high temperature β-$La_2Mo_2O_9$ phase is thus observed in this work.

In order to determine the morphology and microstructure of the powders obtained and to estimate if the crystallite size measured by XRD corresponds to monocrystallized grains or to particles composed of different crystalline domains, the powders have been observed by SEM (Fig. 6) and TEM (Fig. 7A). After a flash heat treatment of 5 min at 500 °C, the powder is composed of platelet particles of few hundred nanometers long and around twenty nanometers thick. This thickness is in agreement with the

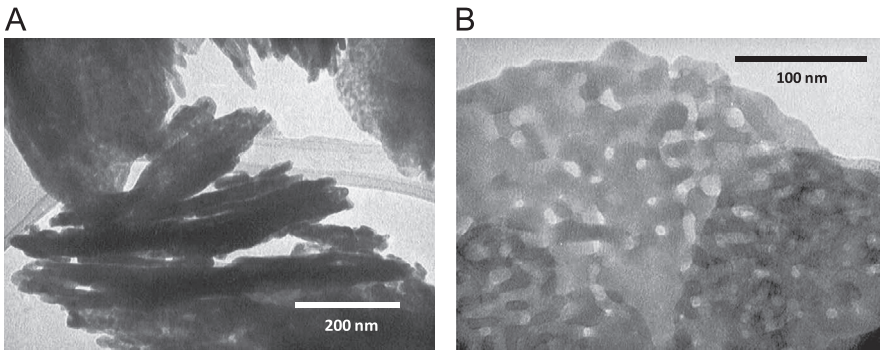

Fig. 7. TEM images of the polyol-process made powders heated at 500 °C for 5 min, (A) observation of platelet particles with different orientations and (B) top view of a platelet particle.

crystallite size determined previously by XRD. For each treatment, the low magnification SEM observations evidence the high level of homogeneity in grain sizes. The observations of these platelet particles by TEM show that they consist of small domains connected to one another, letting holes between them during the heat treatment (Fig. 7B). When two platelet particles stick together the holes are not necessarily aligned. Selected area electron diffraction (SAED) performed on numerous, either isolated or superimposed, platelet particles indicates that the domains that build up the particles are slightly disoriented, as well as the platelet particles relative to each others.

No well defined crystallites are distinguished. However, it can be pointed out that the thickness of the platelet particles is in accordance with the large FWHM of the XRD peaks. By increasing annealing time and temperature, platelet particles sinter until they form large grains of a few micrometers size after a heat treatment at 950 °C, leading to narrow XRD peaks, in agreement with a large crystallite size.

3.2. Effect of the solvent

Different polyols have been used in order to determine their effect on the grain morphology of the prepared powders. In this section, we focus on powders obtained after a flash heat treatment at 500 °C for 2 h, such a duration allowing an easier observation of possible impurities.

Pure $La_2Mo_2O_9$ is obtained with DEG whereas $La_2Mo_3O_{12}$ impurity is observed by XRD when used solvent is EG, PEG or TEG (Fig. 8). The amount of $La_2Mo_3O_{12}$ impurity is higher with TEG. The purity of $La_2Mo_2O_9$ obtained with DEG was confirmed by XRD of the precursor heated at higher temperature.

3.3. Effect of microwave assistance

The aim of this section is to determine the effect of microwave assistance on the purity and the grain morphology of the precipitate after a heat treatment at 500 °C. The microwave assistance has already been successfully used particularly for the synthesis of doped ZnO nanocrystals [23].

All the powders obtained using microwave assistance and a heat treatment at 500 °C for 2 h are identified to be pure $La_2Mo_2O_9$ when EG as well as any other of the polyols are used as solvent (Fig. 9). This result is thus very important, since the microwave

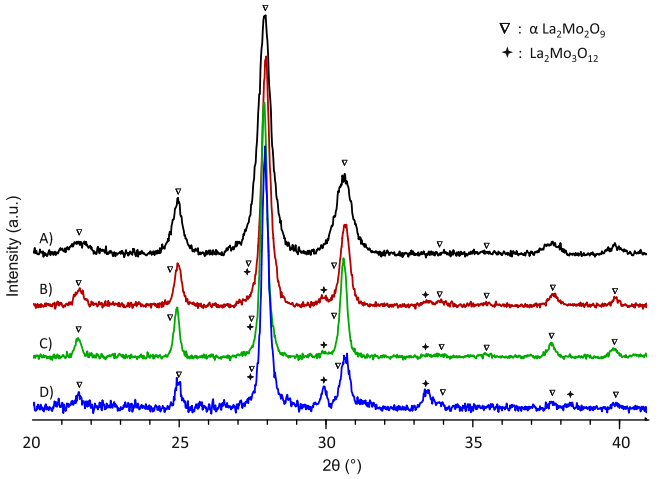

Fig. 8. XRD diagrams of the polyol-process made powders in (A) DEG, (B) EG, (C) PEG and (D) TEG heated at 500 °C for 2 h.

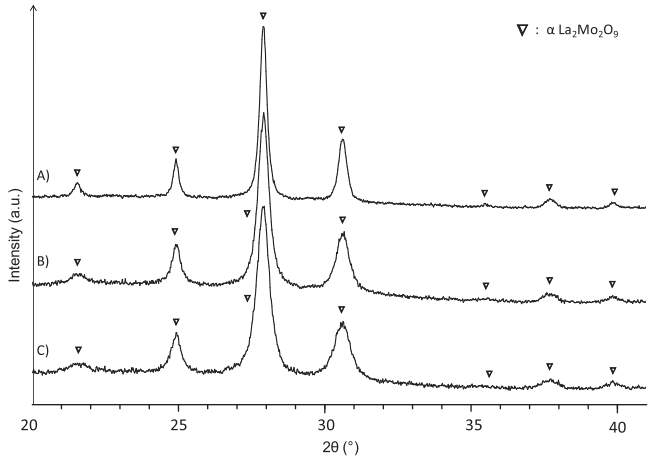

Fig. 9. XRD diagrams of the powders obtained by the microwave assisted polyol processes with (A) EG, (B) DEG and (C) by the classical polyol process with DEG, heated at 500 °C for 2 h.

assistance allows the preparation of pure $La_2Mo_2O_9$ from the solvent with the lower relative toxicity, namely EG.

SEM observations evidence a strong difference in morphology when the microwave assistance is used (Fig. 10). Large porous and monodispersed grains (more or less 1 μm in diameter) are observed. Some long and thin crystallites are present at the

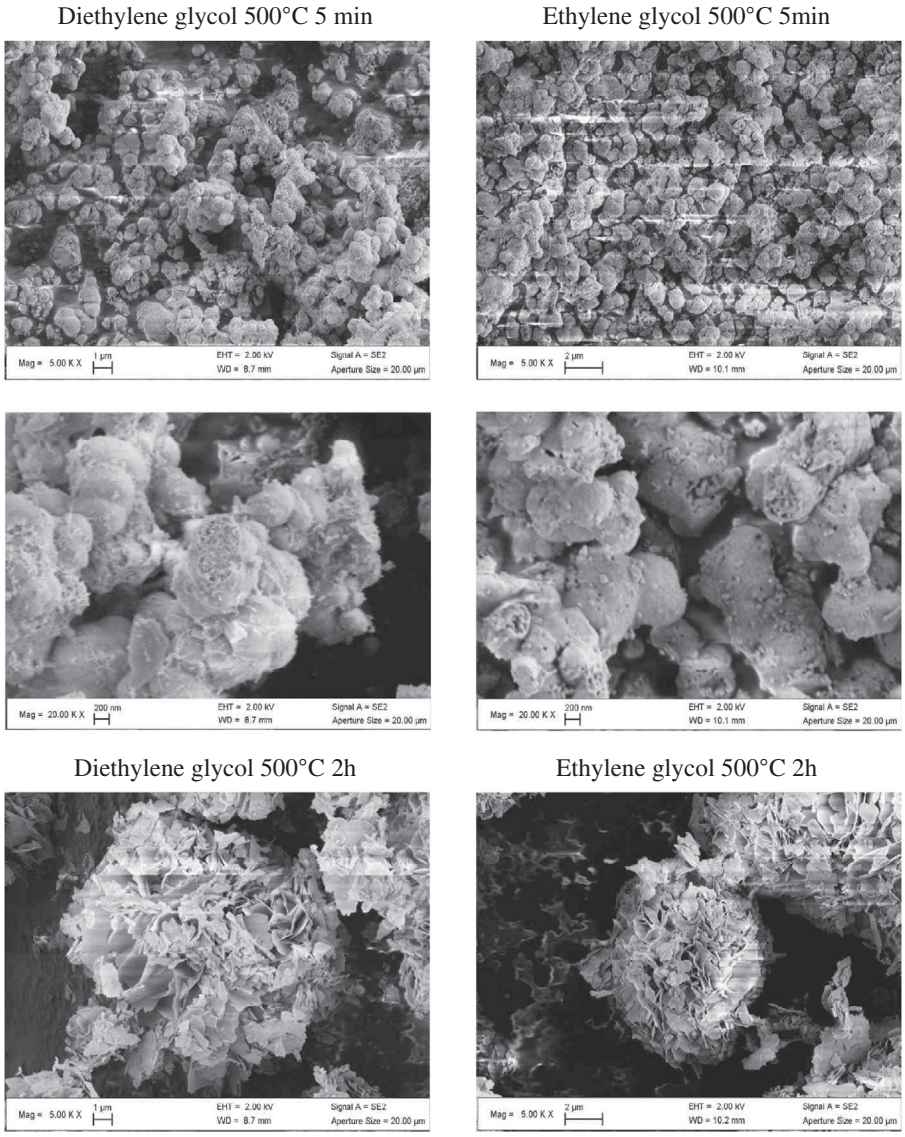

Fig. 10. SEM images of the powders obtained with microwave assistance with DEG and EG heated at 500 °C for 5 min and 2 h.

surface of the grains, and form desert-rose like agglomerates. Moreover, with the microwave assistance, an important evolution of the morphology is observed after a heat treatment at 500 °C for 2 h compared to 5 min: it seems that the crystallites grow during the heat treatment to give, after 2 h, far larger desert roses (around 10 times bigger). This is far different from the classical polyol process for the study made with DEG since in these conditions, no important evolution of the morphology was observed. In addition, by varying the solvent (EG or DEG), the morphology and its evolution with the heat treatment time are similar.

3.4. Effect of the different parameters on the specific surface area

The specific surface area, according to the BET method, of the precursors obtained by the classical and the microwave assisted processes with DEG, and by the microwave assisted process with EG and flash heat treatment at 500 °C for 5 min, was measured (Table 1). Powders prepared by microwave assistance in DEG exhibit a slightly higher specific surface area. However, in EG, the specific surface area is similar to that obtained with the classical polyol process. This should allow measuring the effect of the morphology on catalysis, the specific surface area being constant.

Table 1
Specific surface area according to the BET method of the precursors obtained by the classical or the microwave assisted processes with EG or DEG and flash heat treated at 500 °C for 5 min.

Sample	Process	Solvent	S_{BET} ($m^2\ g^{-1}$)
P_{DEG}	Polyol	DEG	24.6 ± 1.2
M_{DEG}	Microwave assisted	DEG	36.0 ± 1.8
M_{EG}	Microwave assisted	EG	23.3 ± 1.2

For comparison, the specific surface areas presented by Kuang et al. [24] for $La_2Mo_2O_9$ powders obtained from citrates reach 21.3 $m^2\ g^{-1}$ with a heat treatment at 500 °C for 4 h. In the current work, powders with slightly higher specific surface area have been prepared at the same temperature in a shorter time by using microwave assisted polyol process with DEG.

4. Conclusions

This work evidences that the polyol process is a simple and efficient way to prepare pure $La_2Mo_2O_9$ materials, without expensive devices. After the dissolution of the starting material, precipitates are formed under reflux. A heat treatment at 500 °C only for a short period of time is necessary to obtain pure materials. This temperature is far lower than that used in the solid state route (around 900–1000 °C). The effects of different parameters (heat treatment temperature and time, nature of the polyol, microwave assistance) on the phase purity, structure and morphology were determined. Agglomerated platelet particles or desert roses composed of nanocrystallites can be obtained. Such morphologies are very promising for applications such as catalysis since they present a high specific surface area, easily reachable by gases. The study of the effect of other parameters used in the polyol process and of the possibility to make cationic substitutions is currently in progress.

Acknowledgments

We would like to acknowledge the Ministère de l'Enseignement Supérieur et de la Recherche Scientifique of the Tunisian Republic and the Ecole Doctorale Matière, Molécule et Matériaux en Pays de la Loire (3MPL) (ED 500) for their financial support.

The authors also express their thanks to Ms. Melanie Joly from the IUT of Le Mans for her help with BET measurements.

References

[1] A.J. Jacobson, Materials for solid oxide fuel cells, Chemical Materials 22 (2010) 660–674.

[2] P. Lacorre, F. Goutenoire, O. Bohnke, R. Retoux, Y. Laligant, Designing fast oxide-ion conductors based on $La_2Mo_2O_9$, Nature 404 (2000) 856–858.

[3] F. Goutenoire, O. Isnard, R. Retoux, P. Lacorre, Crystal structure of $La_2Mo_2O_9$, a new fast oxide-ion conductor, Chemical Materials 12 (2000) 2575–2580.

[4] F. Goutenoire, O. Isnard, E. Suard, O. Bohnke, Y. Laligant, R. Retoux, Ph. Lacorre, Structural and transport characteristics of the LAMOX family of fast oxide-ion conductors, based on lanthanum molybdenum oxide $La_2Mo_2O_9$, Journal of Materials Chemistry 11 (2001) 119–124.

[5] J. Jacquens, D. Farrusseng, S. Georges, J.-P. Viricelle, C. Gaudillère, G. Corbel, P. Lacorre, Tests for the use of $La_2Mo_2O_9$-based oxides as multipurpose SOFC core materials, Fuel Cells 10 (2010) 433–439.

[6] J.E. Vega-Castillo, U.K. Ravella, G. Corbel, P. Lacorre, A. Caneiro, Thermodynamic stability, structural and electrical characterization of mixed ionic and electronic conductor $La_2Mo_2O_{8.96}$, Dalton Transactions 41 (2012) 7266–7271.

[7] X.C. Lu, J.H. Zhu, Amorphous ceramic material as sulfur-tolerant anode for SOFC, Journal of Electrochemistry Society 155 (2008) B1053–B1057.

[8] D. Marrero-López, J. Canales-Vázquez, J.C. Ruiz-Morales, A. Rodríguez, J.T.S. Irvine, P. Núñez, Synthesis, sinterability and ionic conductivity of nanocrystalline $La_2Mo_2O_9$ powders, Solid State Ionics 176 (2005) 1807–1816.

[9] S. Georges, R.A. Rocha, E. Djurado, Microstructure related conductivity in $La_2Mo_2O_9$ ceramics, Journal of Physics and Chemistry C 112 (2008) 3194–3202.

[10] D. Marrero-López, J. Peña-Martínez, D. Pérez-Coll, P. Núñez, Effects of preparation method on the microstructure and transport properties of $La_2Mo_2O_9$ based materials, Journal of Alloys Compd 422 (2006) 249–257.

[11] Z. Zhuang, X.P. Wang, A.H. Sun, Y. Li, Q.F. Fang, Sol–gel synthesis and transport property of nanocrystalline $La_2Mo_2O_9$ thin films, Journal of Sol–Gel Sciences and Technology 48 (2008) 315–321.

[12] R. Subasri, D. Matusch, H. Näfe, F. Aldinger, Synthesis and characterization of $(La_{1-x}M_x)_2Mo_2O_{9-\delta}$; M=$Ca^{2+}$, Sr^{2+} or Ba^{2+}, Journal of the European and Ceramic Society 24 (2004) 129–137.

[13] Z. Zhuang, X.P. Wang, D. Li, T. Zhang, Q.F. Fang, Ionic conductivity enhancement of $La_2Mo_{2-x}W_xO_9$ nanocrystalline films deposited on alumina substrates by the Sol–-Gel method, Journal of the American Ceramic Society 92 (4) (2009) 839–844.

[14] J.X. Wang, X.P. Wang, F.J. Liang, Z.J. Cheng, Q.F. Fang, Enhancement of conductivity in $La_2Mo_2O_9$ ceramics fabricated by a novel three-stage thermal processing method, Solid State Ionics 177 (2006) 1437–1442.

[15] T. Saradha, S. Muzhumathi, A. Subramania, Microwave-assisted combustion synthesis of nanocrystalline $La_2Mo_2O_9$ oxide-ion conductor and its characterization, Journal of Solid State Electrochemistry 12 (2008) 143–148.

[16] H. Cheng, H. Wang, L. Li, Z. Lu, D. Qian, Facile synthesis of $La_2Mo_2O_9$ nanoparticles via an EDTA complexing approach, Rare Metals 27 (2008) 340–344.

[17] D. Larcher, G. Sudant, R. Patrice, J.-M. Tarascon, Some insights on the use of polyols-based metal alkoxides powders as precursors for tailored metal-oxides particles, Chemical Materials 15 (2003) 3543–3551.

[18] S.D. Škapin, I. Sondi, Synthesis and characterization of calcite and aragonite in polyol liquids: control over structure and morphology, Journal of Colloid Interface and Sciences 347 (2010) 221–226.

[19] R. Justin Joseyphus, B. Jeyadevan, Low temperature synthesis of ITO nanoparticles using polyol process, Journal of Physics and Chemistry of solids 72 (2011) 1212–1217.

[20] M.A. Flores-Gonzalez, G. Ledoux, S. Roux, K. Lebbou, P. Perriat, O. Tillement, Preparing nanometer scaled Tb-doped Y_2O_3 luminescent powders by the polyol method, Journal of Solid State Chemistry 178 (2005) 989–997.

[21] S. Georges, F. Goutenoire, Y. Laligant, P. Lacorre, Reducibility of fast oxide-ion conductors $La_{2-x}R_xMo_{2-y}W_yO_9$ (R=Nd, Gd), Journal of Materials and Chemistry 13 (2003) 2317–2321.

[22] G. Corbel, Y. Laligant, F. Goutenoire, E. Suard, P. Lacorre, Effects of partial substitution of Mo^{6+} by Cr^{6+} and W^{6+} on the crystal structure of the fast oxide-ion conductor $La_2Mo_2O_9$, Chemical Materials 17 (2005) 4678–4684.

[23] E. Hammarberg, A. Prodi-Schwab, C. Feldmann, Microwave-assisted polyol synthesis of aluminium- and indium-doped ZnO nanocrystals, Journal of Colloid Interface ans Sciences 334 (2009) 29–36.

[24] W. Kuang, Y. Fan, K. Yao, Y. Chen, Preparation and characterization of ultrafine rare earth molybdenum complex oxide particles, Journal of Solid State Chemistry 140 (1998) 354–360.